

Numerical Investigation of inlet distortion on the flowfield within the NASA rotor67

HengMing Zhang¹, XiuQuan Huang¹, Xiang Zhang¹, QingZhen Yang¹

¹(School of power and energy, Northwestern Polytechnical University, China)

ABSTRACT: Based on Harmonic Balance method, this paper studies the effect of inlet distortion on the performance of NASA Rotor67. Two kinds of inlet distortion with different sinusoidal forms of circumferential total pressure distribution have been applied on the inflowing boundary. The numerical results show that the solver based on frequency domain is capable of simulating the nonuniform flow in circumferential direction and can capture the detailed propagation of inlet distortion in the blade passage very well. The analysis shows that low frequency inlet distortion lead to a higher loss, while both inlet distortion have the similar total pressure ratio characteristic. There is little difference in stall margin of compressor for two types of inlet distortion. And for both types of inlet total pressure distribution, the low total pressure inlet zone is the source of high intension of tip clearance flow which results in the entropy production.

Keywords - Inlet distortion, Rotor67, Harmonic balance, Unsteady flow, Performance

I. INTRODUCTION

Inlet distortion is very common in the actual flight of the aircraft and tends to be inevitable, e.g., the changing of flight attitude and flow separation in inlet duct. The nonuniform inlet flow can lead to performance degradation of fan/compressor. The studies about inlet distortion can be traced back to the middle of last century[1]. In earlier studies, experiments and simplified models were applied on researches about the effects of interaction between inlet distortion and compressor/fan. For instance, comparing with experimental results, Korn validated the reliability and accuracy of "parallel compressor" model in predicting inlet distortion induced stall[2]. And the results showed that this model agreed well with circumferential distortion test data on the single compressor stage, while it failed being used to estimate the multistage compressor. To investigate the effects of the inlet distortion on compressor stability, a series of experiments have been conducted by Greitzer[3]-[5]. Until the 90s of last century, some researchers began to exploit the Computational Fluid Dynamics(CFD) to study the inlet distortion of compressor/fan. For instance, combining CFD technique, Joubert[6] established two method to predict the compressor/fan inlet distortion. One method adopted two-dimension Euler unsteady calculation, another method combined "actuator disks" method and three-dimension Euler calculation. His analysis demonstrated that it was necessary for prediction of inlet distortion to establish study on three-dimension numerical simulation and "actuator disks" ignored the detailed flowfield in the blade. To control the inlet distortion induced compressor stall, the effect of casing treatment on inlet distortion has been investigated experimentally by Dong[7]. And The stall margin enhancement with a kind of stall precursor-suppressed (SPS) casing treatment has been found in their experiments.

Many researches about inlet distortion of compressor/fan have been completed by experiments and some simplified models. But few studies were completed by numerical simulation due to the very high computation cost, though the unsteady Reynold-averaged Navier-Stokes computation technique nowadays is mature and reliable for the researches about inlet distortion. To reduce calculation amount, the Hamornic Balance(HB) method[8] based on frequency domain has been adopted in this paper. And the numerical investigation of inlet distortion on the performance of compressor has been presented.

II. COMPUTATIONAL APPROACH

The model equation of HB method is derived from the unsteady Reynolds Averaged Navier-Stokes equations(U-RANS). The integrated U-RANS equations could be expressed as follow:

$$\frac{\partial}{\partial t} \iiint_{\delta V} U dV + \iint_{\delta A} (F - Uv_{mg}) \cdot ndA = \iiint_{\delta V} (S_i + S_v) dV \tag{1}$$

Where, U are the conservative variables, F are the convective terms, Uv_{mg} are the flux terms from the grid moving, S_i are the centrifugal source terms and S_v are the viscous terms. The basic idea of Harmonic balance method is that the conservative variables could be decomposed into a time-averaged value and a sum of periodic perturbations, expressed as the fourier series form:

$$U = U_0 + \sum_{n=1}^N (A_n \sin(\omega_n t) + B_n \cos(\omega_n t)) \tag{2}$$

U_0 is the zero-order fourier coefficient, which represents the time-averaged value of conservative variables. And A_n and B_n are the N'th order fourier coefficient, ω_n is the N'th angular frequency respect to A_n and B_n . U^* is a vector which consists of $2N+1$ samples corresponding to different time, and \tilde{U} is the vector of fourier coefficients.

$$U^* = E \tilde{U} \tag{3}$$

Where, $U^* = [U_1 \ U_2 \ U_3 \ \dots \ U_{2N} \ U_{2N+1}]^T$

$$\tilde{U} = [U_0 \ A_1 \ B_1 \ \dots \ A_N \ B_N]^T$$

E is the fourier matrix. And substituting Eq. 3 into Eq.1, the governing equations could be derived as follow:

$$\frac{\partial}{\partial \tau} \iiint_{\delta V} U^* dV + \iint_{\delta A} (F^* - U^* v_{mg}) \cdot ndA = \iiint_{\delta V} (S_i^* + S_v^* + DU^*) dV \tag{4}$$

Where, $DU^* = \frac{\partial E}{\partial t} E^{-1} U^*$, D is the frequency domain operator.

Eq(4) is the final set of equations that this article would to solve. So the number of simultaneous equations for HB method is $2N+1$. By employing the phase-lag boundary condition, the HB unsteady calculation can be conducted on a single-passage mesh. As a result, the amount of unsteady computation is as $2N+1$ as that of steady. The accuracy and stability of HB method has been validated by Gopinath [9].

As for the numerical method, the central difference method with second-order accuracy and lower-upper symmetric Gauss-Seidel (LU-SGS) implicit time integration have been applied in this article. In order to reduce time cost, local time stepping, implicit residual smoothing and multigrid techniques are employed to accelerate convergence. The one-equation S-A model is chosen as turbulence model to calculate turbulence viscosity coefficient, which is widely used in turbomachinery numerical simulation.

III. TEST CASE AND VALIDATION

The test case in this paper is NASA Rotor67. It is a transonic compressor rotor. And because the detailed experimental data of Rotor67 could easily be found in the NASA technical report[9], Rotor 67 becomes one of the most popular research objects in turbomachinery field. The design parameters of NASA Rotor67 are showed in table 1.

Table 1. NASA Rotor67 Design Parameters

Number of Blade		22
Blade Speed(rpm)		16043
Massflow(kg/s)		33.25
Total Pressure Ratio		1.63
Tip Speed(m/s)		429
Tip Mach Number		1.38
Aspect Ratio		1.56
Solidity	Tip	3.11
	Root	1.29
Hub-to-tip Radii Ratio	Inlet	0.375
	Outlet	0.478
Blade Tip Diameter(cm)	Inlet	51.4
	Outlet	48.5

Because of the adoption of phase-lag condition, the single passage grid could be used in the numerical simulation. The H-type mesh topology has been applied to generation of grid. The grid number of Rotor67 is

about 5.4×10^6 with 65 grid points at radial direction, which is more enough to meet the requirement of grid independence. The blade-to-blade grid and validation of mesh independence has been showed in Fig.1

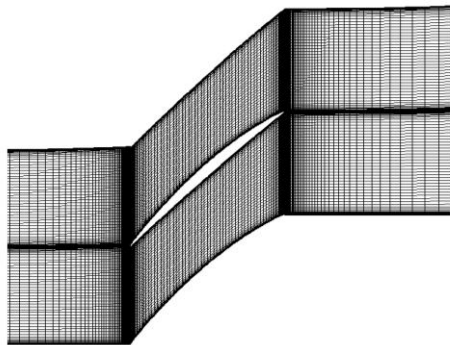
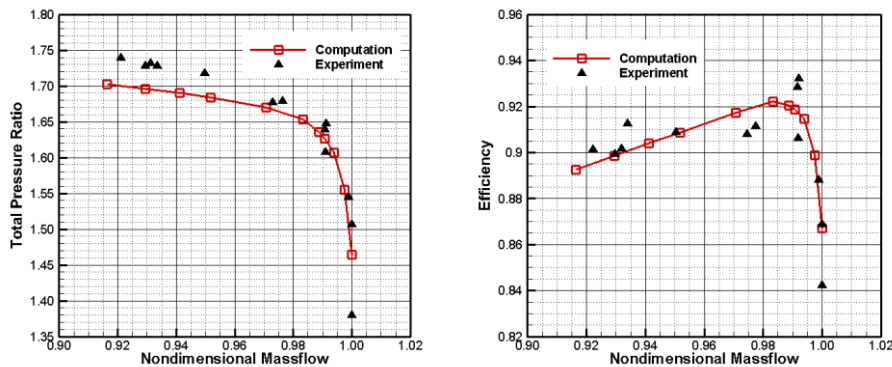


Figure 1. Grid at blade-to-blade surface

To make sure the numerical simulation results reliable, it is necessary to compare the numerical and experimental data. Fig. 2 shows the total pressure ratio characteristic and efficiency characteristic.



(a) total pressure ratio characteristic

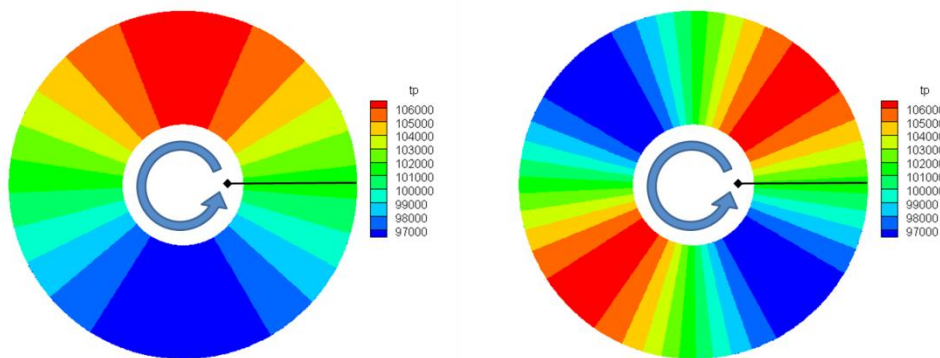
(b) efficiency characteristic

Figure 2. Rotor67 characteristics: experiment and computation

It is clear that the total pressure ratio of numerical simulation near stall boundary is little lower than that of experiment. However, the trend of computation is coincident with experiment. Also, the efficiency characteristic curve of computation agrees well with experimental results. So the numerical method and the solver adopted in this article are credible and trustworth.

IV. RESULTS

Adopting the mesh described above, two unsteady simulations based on harmonic balance method have been proceeding with two kinds of sinusoidal inlet distortion respectively. The inlet total pressure distribution contour are displayed in Fig.3.



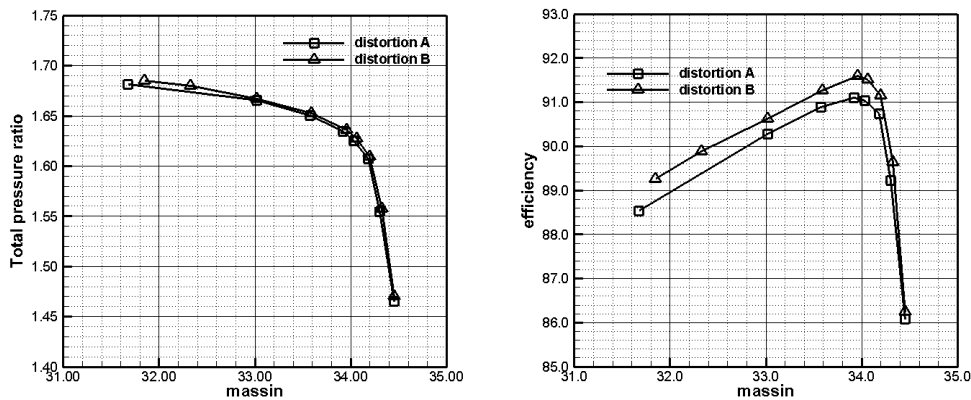
(a) distortion A

(b) distortion B

Figure 3. Inlet total pressure distribution: distortion A and distortion B

For two kinds of inlet distortion, the variations of amplitude are both 5 percentages of atmospheric pressure(101325pa) and the averaged inlet total pressure are both 101325pa. So the only different between two inlet distortion forms is the frequency. For distortion A, Rotor67 would experience one period when it rotates one revolution around its axis. And for distortion B, two sinusoidal waves sweep the blades during one revolution.

Fig. 4 compares the Rotor67 performances from distortion A and distortion B numerical simulations at designed rotational speed. It is clear that the total pressure ratio characteristic curve of distortion A agrees well with that of distortion B, while the differences of efficiency characteristic between distortion A and distortion B is obvious. Specifically, at choked operating point, the efficiency of distortion A and distortion B is nearly the same. However, with the operating point toward stall boundary, the efficiency of distortion B is higher than that of distortion A and this tendency is increasingly apparent.



(a) total pressure ratio characteristic (b) efficiency characteristic
 Figure 4. Rotor67 characteristics: distortion A and B

Entropy is often used to characterize the loss in turbomachinery flow study. So to know more about the rotor response to inlet distortion and deepen understanding about the interaction mechanism between the inlet distortion and blade flowfield, the instantaneous entropy distributions for both distortion forms at 99% span at near design operating point are presented in Fig. 5.

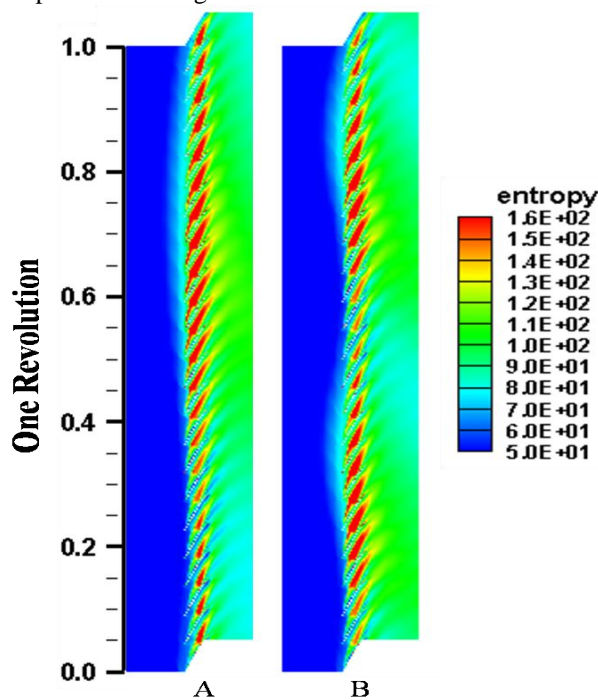


Figure 5. Entropy instantaneous distribution at the 99% spanwise location at design condition

Fig. 5 shows that the variations of entropy in a full annular of both distortion forms are also sinusoidal, which keep consistent with their inlet distortion waves. So the sinusoidal form inlet distortion lead to an almost sinusoidal form variation of flowfield.

Specially, it is easy to recognize that the stripy high entropy area in Fig.5 is due to the tip clearance flow. So the intensity of tip leakage is changing with time in sine form.

Also, combining the Fig. 5 and Fig. 3, it could be found that the high entropy areas in Fig. 5 are corresponding to the low total pressure areas in Fig. 3, which indicates that low total pressure inlet could lead to loss increment.

V. CONCLUSION

Harmonic balance method could be used to numerical simulate inlet distortion efficiently and reliably. By HB technique, the NASA Rotor67 encountering two kinds of sinusoidal inlet distortion with different frequencies has been investigated. The results demonstrate that the frequency of inlet distortion has considerable influence on efficiency of Rotor67, while its impact on stall margin of Rotor67 is limited. Additionally, low pressure domain of inflowing boundary could strengthen the tip clearance massflow and lead to obvious entropy production. And the effects would be more significant for low frequency inlet distortion.

REFERENCES

- [1] Conrad, E. William, and Adam E. Sobolewski, Investigation of Effects of Inlet-Air Velocity Distortion on Performance of Turbojet Engine, 1950.
- [2] Korn, James A, Compressor Distortion Estimates Using Parallel Compressor Theory and Stall Delay, *Journal of Aircraft*, 11(9), 1974, 584-586.
- [3] Callahan G M, Stenning A H, Attenuation of inlet flow distortion upstream of axial flow compressors, *Journal of Aircraft*, 8(4), 1971, 227-233.
- [4] Horlock J H, Greitzer E M, Henderson R E, The response of turbomachine blades to low frequency inlet distortions, *Journal of Engineering for Power*, 99(2) , 1977, 195-203.
- [5] Hynes T P, Greitzer E M, A method for assessing effects of circumferential flow distortion on compressor stability, *Journal of Turbomachinery*, 109(3), 1987, 371-379.
- [6] Joubert H, Flowfield calculation in compressor operating with distorted inlet flow, *ASME 1990 International Gas Turbine and Aeroengine Congress and Exposition*. American Society of Mechanical Engineers, Brussels, Belgium, 1990, V001T01A065-V001T01A065
- [7] Dong X, Sun D, Li F, et al, Effects of Rotating Inlet Distortion on Compressor Stability With Stall Precursor-Suppressed Casing Treatment. *Journal of Fluids Engineering*, 137(11) , 2015, 111101.
- [8] Hall K C, Thomas J P, Clark W S, Computation of unsteady nonlinear flows in cascades using a harmonic balance technique, *AIAA journal*, 40(5), 2002, 879-886.
- [9] Gopinath A, Van Der Weide E, Alonso J J, et al. Three-dimensional unsteady multi-stage turbomachinery simulations using the harmonic balance technique[C]//45th AIAA Aerospace Sciences Meeting and Exhibit. 2007, 892.